Syntheses and Electrochemical, Photophysical, and Photochemical Properties of Ruthenium(II) 4,5-Diazafluorenone Complexes and Their Ketal Derivatives

Youxiang Wang, Willie Perez, Greg Y. Zheng, and D. Paul Rillema*

Department of Chemistry, Wichita State University, Wichita, Kansas 67260-0051

Received August 7, 1997

A series of ruthenium(II) complexes of the types $[Ru(bpy)_n(dafo)_{3-n}]^{2+}$ and $[Ru(bpy)_n(dafo\text{-}ketal)_{3-n}]^{2+}$, where *n* varies between 0 and 3 and dafo is 4,5-diazafluoren-9-one, were synthesized, and their chemical, physical, and photophysical properties were examined. The coordinated dafo-ketal ligand readily forms by the direct reaction of $[Ru(bpy)_n(dafo)_{3-n}]^{2+}$ complexes with ethylene glycol or by reaction of the appropriate ruthenium precursors with the correct stoichiometric amount of the dafo ligand in ethylene glycol. In each series, the visible absorption band associated with the MLCT transition shifts to the blue and the electrochemical oxidation associated with the Ru(III)/Ru(II) couple becomes more positive as *n* decreases. Coordinated dafo undergoes a one-electron reduction at potentials <-1 V and a second one-electron reduction at ~-1.2 V vs SSCE. The first reduction can be associated with reduction of the carbonyl group; the second, with reduction of the bipyridine portion. Coordinated dafo-ketal only reduces at potentials <-1.2 V. The emission properties place the emitting state of the complexes on the bipyridine portion of the dafo ligand, not the carbonyl group. At 77 K in a 4:1 ethanol−methanol glass, the emission lifetimes fall in a range of 5−2 μs as *n* decreases. In fluid solution, the emission lifetimes are temperature dependent with activation energies that vary from 1400 to 500 cm^{-1} as *n* decreases. The thermally accessible state is assigned as a fourth metal-to-ligand charge transfer (MLCT″) state since the compounds are photochemically unreactive.

Introduction

There is currently an increasing interest in luminescent and redox-reactive transition-metal complexes, especially in view of their use as building blocks for the design of photochemical molecular devices that perform useful light-induced functions such as energy migration and charge separation.[1] Ruthenium(II) polypyridine-type complexes exhibit suitable excited-state and redox properties to play the role of building blocks for the construction of photoactive supramolecular systems.[2] For synthetic reasons, however, it is quite difficult to assemble these metal-containing building blocks because the synthesis of covalently linked ligands used in the preparation of multimetallic complexes is tedious and lacks versatility. Therefore, one of the goals in our laboratories is to find a way to simplify the synthetic work. Thus, we have turned our attention to preparing polypyridyl ligands with reactive chemical sites. One of the special ligands is 4,5-diazafluorenone (dafo). This special ligand has several distinct properties compared to its analogue 2,2′-bipyridine. First, it contains a reactive exocyclic ketone. Second, the rigid structure imposed by the central five-member ring means that the two nitrogen atoms are always held in the same direction. Third, strain will be generated in the central five-member ring once it coordinates to ruthenium(II).

Our experimental results have shown that coordinated dafo has reactivity quite different from that of the free ligand. For example, a novel ring-opening reaction occurs with certain nucleophiles, such as hydroxide ion, ethoxide ion, and pyridine derivatives, resulting in 3′-substituted bipyridine ligands,[3] but the free ligand only undergoes Schiff base condensation reactions.[4] DBU (1,8-diazabicyclo[5.4.0]undec-7-ene) also reacts as a nucleophile[5] with coordinated dafo, opens the five-member ring, but, in contrast to other amines which act as catalysts, remains bonded to the ring-opened ligand.[6]

In this paper we focus on the syntheses and properties of a series of ruthenium(II) complexes of the types $[Ru(bpy)_n(dafo)_{3-n}]^{2+}$ and $[Ru(bpy)_n(dafo\text{-}ketal)_{3-n}]^{2+}$, where *n* varies between 0 and 3, whose structures are shown in Figure 1. For some of the dafo complexes, the usual procedures to prepare ruthenium complexes of heterocyclic ligands required modification due to the reactivity of the exocyclic ketone on the dafo ligand which generated stable ketals that did not hydrolyze as normally found for organic compounds.[7]

(1) (a) *Supramolecular Photochemistry*; Balzani, V., Ed.; NATO ASI Series; Reidel: Dordrecht, The Netherlands, 1987. (b) Meyer, T. J. *Acc. Chem. Res.* **1989**, *22*, 163. (c) *Supramolecular Photochemistry*; Balzani, V., Scandola, F., Eds.; Horwood: Chichester, U.K., 1990.

(2) (a) Balzani, V.; Juris, A.; Venturi, M.; Campagna, S.; Serroni, S. *Chem. Rev.* **1996**, *96*, 759. (b) Balzani, V.; Ballardini, R.; Bolleta, F.; Gandolfi, M. T.; Juris, A.; Maestry, M.; Mamfrin, M. F.; Moggi, L.; Sabbatini, N. *Coord. Chem. Rev.* **1993**, *113*, 227. (c) Juris, A.; Balzani, V.; Barigelletti, F.; Campagna, S.; Belser, P.; Von Zelewsky, A. *Coord. Chem. Rev.* **1988**, *84*, 85. (d) Ghosh, B. K.; Chakravorty, A. *Coord. Chem. Rev.* **1985**, *95*, 239. (e) DeArmond, M. K.; Carlin, C. M. *Coord. Chem. Rev.* **1981**, *36*, 325.

(3) (a) Zheng, G. Y.; Wang, Y.; Rillema, D. P. *Inorg. Chem.* **1996**, *35*, 7118. (b) Wang, Y.; Rillema D. P. *Tetrahedron Lett.* **1997**, *38*, 6627.

(4) (a) Tai, Z.; Zhang, G.; Qian, X. *Langmuir* **1993**, *9*, 1601. (b) Xia, X.; Duang, C.; Zhu, L.; You, X. *Polyhedron* **1992**, *11*, 1917. (c) Wang, Y.; Rillema, D. P. *Tetrahedron* **1997**, *53*, 12377.

(5) (a) Lammers, H.; Cohen-Fernandes, P.; Habraken, C. L. *Tetrahedron* **1994**, *50*, 865. (b) McCoy, L. L.; Mal, D. *J. Org. Chem.* **1981**, *46*, 1016. (c) Perbost, M.; Lucas, M.; Chavis, C.; Imbach, J.-L. *J. Heterocycl. Chem.* **1993**, *30*, 627. (d) Chambers, R. D.; Roche, A. J.; Batsanov, A. S.; Howard, J. A. K. *J. Chem. Soc., Chem. Commun.* **1994**, 2055. (e) Reed, R.; Reau, R.; Dahan, F.; Bertrand, G. *Angew. Chem., Int. Ed. Engl.* **1993**, *32*, 399. (f) Ma, L.; Dolphin, D. *J. Chem. Soc., Chem. Commun.* **1995**, 2251.

(6) Wang, Y.; Rillema, D. P. *Inorg. Chem. Commun.*, in press.

S0020-1669(97)00987-7 CCC: $15.00
Published on Web 04/03/1998

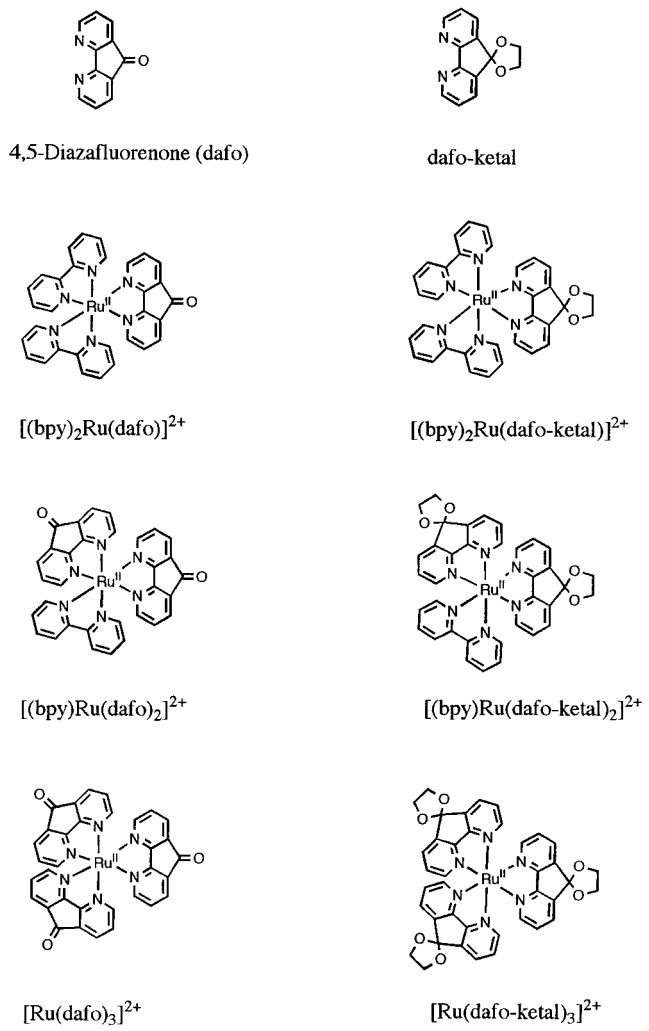

Figure 1. Structures of the ligands and complexes.

Experimental Section

Materials. All reagents and solvents were purchased commercially as HPLC grade and were used without further purification unless otherwise noted. Acetonitrile was dried over 3 Å activated molecular sieves prior to use. Commercially purchased tetrabutylammonium hexafluorophosphate (TBAH) was of electrometric grade (Southwestern Analytical, Inc.) and was used without further purification. The following compounds were prepared according to literature methods: 4,5-diazafluoren-9-one (dafo),[8] $Ru(bpy)_2Cl_2 \cdot 2H_2O$,[9] and $Ru(bpy)_2CO_3 \cdot 2H_2O$.[10]

Preparation of $[(bpy)_2Ru(dafo)](PF_6)_2$. *cis*-$Ru(bpy)_2Cl_2 \cdot 2H_2O$ (0.52 g, 1 mmol) and dafo (0.18 g, 1 mmol) were refluxed in 23 mL of ethanol for about 5 h. The solution was filtered hot, and NH_4PF_6 (0.78 g) was added. After the solution stood overnight in a refrigerator, crystals of $[(bpy)_2Ru(dafo)](PF_6)_2$ precipitated. The compound was dissolved in water, the resulting solution was loaded onto a cation exchange chromatography column (Sephadex SP-C25, pharmacia, 40−120 μm), and the complex was eluted with an aqueous solution of HCl. The fraction obtained with 0.2 M HCl was collected, and the complex was precipitated by adding a saturated aqueous solution of NH_4PF_6. The complex was recrystallized in water. The overall yield was 0.70 g (70%). The complex decomposes at 230−231 °C. IR: 1744 (C═O), 1504, 1424 (C═C, C═N), 845, 759 cm^{-1}. Anal. Calcd for $RuC_{31}H_{22}F_{12}N_6OP_2$: C, 42.04; H, 2.51; N, 9.49. Found: C, 42.15; H, 2.46; N, 9.48.

Preparation of $[Ag(dafo)_2]NO_3 \cdot 2H_2O$. Silver nitrate (0.60 g, 3.5 mmol) and dafo (1.29 g, 7 mmol) were added to 80 mL of 50% aqueous ethanol, and the reaction mixture was boiled for 30 min. The solution was allowed to cool to room temperature, and the resulting yellow needles of $[Ag(dafo)_2]NO_3 \cdot 2H_2O$ were collected and washed with a small volume of water. The product was then recrystallized from hot 50% aqueous ethanol and dried in vacuo; yield 1.80 g, 90%. The compound was characterized by IR and NMR spectroscopies.

Preparation of $[(bpy)Ru(dafo)_2](PF_6)_2$. $Ru(bpy)Cl_4$ (0.050 g, 0.125 mmol) and $[Ag(dafo)_2]NO_3 \cdot 2H_2O$ (0.357 g, 0.550 mmol) were refluxed in 20 mL of methanol for about 5 h. The solution was filtered hot and washed with a small amount of methanol three times. The filtrate was rotary-evaporated to dryness and redissolved in a small amount of distilled water. The resulting solution was loaded onto a cation exchange chromatography column (Sephadex SP-C25, pharmacia, 40−120 μm), and the complex was eluted with an aqueous solution of HCl. The fraction obtained with 0.2 M HCl was collected, and the complex was precipitated by adding a saturated aqueous solution of NH_4PF_6. The overall yield was 0.093 g (82%). IR: 1741 (C═O), 1579, 1425 (C═C, C═N), 845, 759 cm^{-1}. Anal. Calcd for $RuC_{32}H_{20}F_{12}N_6O_2P_2$: C, 42.16; H, 2.22; N, 9.22. Found: C, 41.90; H, 2.13; N, 9.04.

Preparation of $[Ru(dafo)_3](PF_6)_2$. $RuCl_3 \cdot xH_2O$ (0.050 g, 0.24 mmol) and dafo (0.153 g, 0.84 mmol) were refluxed in a mixture of 10 mL of ethanol and 10 mL of nitrobenzene for 3 days. The resulting solution was cooled to room temperature and filtered. The filtrate was added dropwise to 350 mL of diethyl ether. The solid was collected by filtration and redissolved in a small amount of distilled water. The solution was loaded onto a cation exchange chromatography column (Sephadex SP-C25, pharmacia, 40−120 μm), and the complex was eluted with an aqueous solution of HCl. The fraction obtained with 0.1 M HCl was collected, and the complex was precipitated by adding a saturated aqueous solution of NH_4PF_6. The overall yield was 0.135 g (60%). IR: 1741 (C═O), 1580, 1425 (C═C, C═N), 840, 750 cm^{-1}. Anal. Calcd for $RuC_{33}H_{18}F_{12}N_6O_3P_2$: C, 42.27; H, 1.94; N, 8.97. Found: C, 42.14; H, 1.82; N, 8.71.

Preparation of $[(bpy)_2Ru(dafo\text{-}ketal)](PF_6)_2$. *cis*-$Ru(bpy)_2Cl_2 \cdot 2H_2O$ (0.10 g, 0.2 mmol) and dafo (0.036 g, 0.2 mmol) were refluxed for about 2 h in 5 mL of ethylene glycol containing a catalytic amount of *p*-toluenesulfonic acid monohydrate. The solution was filtered hot, and a saturated aqueous solution of NH_4PF_6 was added. After the solution stood overnight in the refrigerator, a solid precipitated. The solid was filtered off and redissolved in warm water (not hot water). The resulting solution was loaded onto a cation exchange chromatography column (Sephadex SP-C25, pharmacia, 40−120 μm), and the complex was eluted with an aqueous solution of NaCl. The fraction obtained with 0.2 M NaCl was collected, and the complex was precipitated by adding a saturated aqueous solution of NH_4PF_6. The overall yield was 0.139 g (75%). IR: 1606, 1465, 1446, 1423 (C═C, C═N), 1163 (C−O), 845, 759 cm^{-1}. Anal. Calcd for $RuC_{33}H_{26}F_{12}N_6O_2P_2$: C, 42.63; H, 2.82; N, 9.04. Found: C, 42.80; H, 2.76; N, 9.07.

Preparation of $[(bpy)Ru(dafo\text{-}ketal)_2](PF_6)_2$. $Ru(bpy)Cl_4$ (0.11 g, 0.28 mmol) and dafo (0.13 g, 0.69 mmol) were refluxed in 15 mL of ethylene glycol with a catalytic amount of *p*-toluenesulfonic acid monohydrate for about 1 h. The solution was filtered hot, and a saturated aqueous solution of NH_4PF_6 was added. After the solution stood overnight in the refrigerator, a precipitate formed. The solid was filtered off and redissolved in warm water (not hot water). The resulting solution was loaded onto a cation exchange chromatography column (Sephadex SP-C25, pharmacia, 40−120 μm), and the complex was eluted with an aqueous solution of NaCl. The fraction obtained with 0.2 M NaCl was collected, and the complex was precipitated by adding a saturated aqueous solution of NH_4PF_6. The resulting compound was loaded onto an alumina column and eluted with a 10:0.5 CH_2Cl_2−MeOH mixture. A bright orange band was collected. The solvent was evaporated by rotary evaporation, and the resulting solid was recrystallized twice from a mixture of toluene and methylene chloride. The

(7) Carey, F. A. *Organic Chemistry*, 2nd ed.; McGraw-Hill: New York, 1992.
(8) Henderson, L. J.; Fronczek, F. R., Jr.; Cherry, W. R. *J. Am. Chem. Soc.* **1984**, *106*, 5876.
(9) Sullivan, B. P.; Salmon, D. J.; Meyer, T. J. *Inorg. Chem.* **1978**, *17*, 3334.
(10) Kober, E. M.; Caspar, J. V.; Sullivan, B. P.; Meyer, T. J. *Inorg. Chem.* **1988**, *27*, 4587.

overall yield was 0.134 g (48%). IR: 1604, 1423 (C═C, C═N), 1280, 1215, 1076 (C−O), 840, 557 cm^{-1}. Anal. Calcd for $RuC_{36}H_{28}F_{12}N_6O_4P_2$: C, 43.25; H, 2.83; N, 8.41. Found: C, 43.12; H, 3.01; N, 8.41.

Preparation of [Ru(dafo-ketal)$_3$](PF$_6$)$_2$. $RuCl_3 \cdot xH_2O$ (0.050 g, 0.24 mmol) and dafo (0.153 g, 0.84 mmol) were refluxed for about 1 h in 5 mL of ethylene glycol containing a catalytic amount of *p*-toluenesulfonic acid monohydrate. The solution was filtered hot, and a saturated aqueous solution of NH_4PF_6 was added. After the solution stood overnight in the refrigerator, the solid that formed was filtered off and redissolved in warm water (not hot water). The resulting solution was loaded onto a cation exchange chromatography column (Sephadex SP-C25, pharmacia, 40−120 μm), and the complex was eluted with an aqueous solution of NaCl. The fraction obtained with 0.2 M NaCl was collected, and the complex was precipitated by adding a saturated aqueous solution of NH_4PF_6. The complex was recrystallized twice from a mixture of toluene and methylene chloride. The overall yield was 0.172 g (67%). IR: 1604, 1421 (C═C, C═N), 1280, 1213, 1076, 1026 (C−O), 841, 557 cm^{-1}. Anal. Calcd for $RuC_{39}H_{30}F_{12}N_6O_6P_2$: C, 43.78; H, 2.83; N, 7.86. Found: C, 43.70; H, 2.90; N, 7.84.

Physical Measurements. Visible−UV spectra were obtained with an OLIS modified Cary 14 spectrophotometer. IR spectra were obtained with a Mattson Cynus 25 FT-IR spectrophotometer and were calibrated with the 1601 cm^{-1} band of polystyrene. Nuclear magnetic resonance spectra were obtained with a Varian XL-300 NMR spectrometer. Differential pulse polarograms were obtained with an EG&G PAR model 263A potentiostat/galvanostat. Coulometry was effected using the above potentiostat and the EG&G PAR model 377 cell system. The electrochemical measurements were made in a typical H-cell using a platinum disk working electrode, a platinum gauze counter electrode, and a standard saturated sodium calomel electrode (SSCE) and controlled with a M-Tech microcomputer. The supporting electrolyte was 0.1 M TBAH. All samples were purged with nitrogen prior to measurement. Emission spectra were obtained for each complex in acetonitrile at room temperature and in 4:1 ethanol−methanol at 77 K with a SPEX Fluorolog 212 spectrofluorometer. All emission spectra were corrected for instrument response. Excited-state lifetimes were determined by exciting the samples at 450 nm using an OPOTEK optical parametric oscillator pumped by a frequency-tripled Nd:YAG laser (Continuum Surlite, run at ≤1.5 mJ/10 ns pulse). Spectral regions were isolated using a Hamamatsu R955 PMT in a cooled housing (−15 °C, Amherst) coupled to an Acton SpectraPro 275 monochromator. Transients were recorded with a LeCroy 9359A digital oscilloscope (1 GS/s). Oscilloscope control and data curve fitting were accomplished with a program developed in-house. All emission samples were prepared in HPLC grade, or better, solvents, filtered through 0.45 μm PTFEE filters, and then freeze−pump−thaw degassed prior to measurement. Errors in measurements are ±1 in the last digit, unless indicated. Variable-temperature emission lifetimes from 90 to 290 K were determined by adding a Cryo Industries EVT cryostat controlled by a Lakeshore 805 temperature controller to the system above. The cryostat was modified in-house by adding a larger copper thermal mass and then calibrated with an auxiliary thermocouple using ice-cold water as the reference junction. This resulted in a temperature accuracy of ±1.6 K over the 90−290 K range. Equation 1 was used to calculate the

$$\Phi_{em} = (\eta_{cmpd}^2/\eta_{std}^2)(A_{std}/A_{cmpd})(I_{cmpd}/I_{std})\Phi_{std} \quad (1)$$

emission quantum yields,[11] where A is the absorbance at the excitation wavelength, I is the integrated emission intensity, and η is the index of refraction of the solvent. Emission quantum yields were calculated relative to $[Ru(bpy)_3]^{2+}$ ($\phi_{std} = 0.089$ at $\lambda_{ex} = 436$ nm) in 4:1 ethanol−methanol.[12]

Evaluation of Temperature-Dependent Emission Data. The temperature-dependent emission lifetimes obtained in 4:1 ethanol−methanol for each complex were plotted versus the absolute temperatures. The temperature-dependent profiles generated for each complex were fit to eq 2 by using the program ORIGIN.[13] In eq 2, k_o is the

$$\tau^{-1} = k_o + k_1 e^{-\Delta E/RT} \quad (2)$$

sum of radiative and nonradiative rate constants and set equal to the observed emission decay rate constant at 77 K. The parameters k_1 and ΔE, which are related to the thermal deactivation process of the emission state, were determined from a curve-fitting analysis of the data.

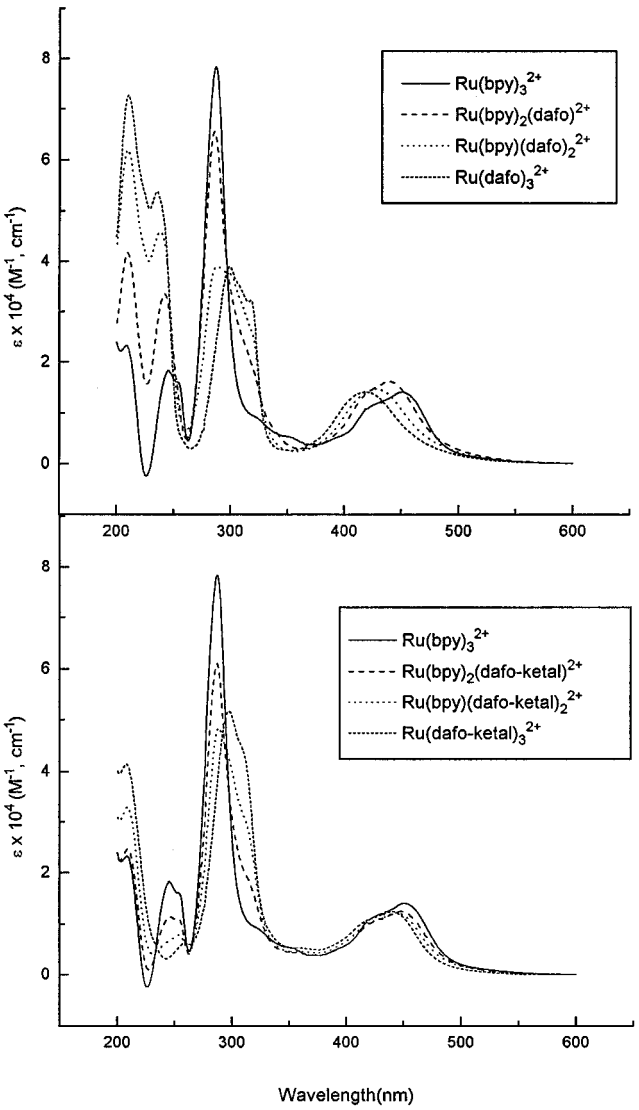

Figure 2. Absorption spectra in acetonitrile solution at room temperature. Top: $Ru(bpy)_3^{2+}$ (solid line), $Ru(bpy)_2(dafo)^{2+}$ (dash line), $Ru(bpy)(dafo)_2^{2+}$ (dotted line), $Ru(dafo)_3^{2+}$ (short dash line). B: $Ru(bpy)_3^{2+}$ (solid line), $Ru(bpy)_2(dafo\text{-}ketal)^{2+}$ (dash line), $Ru(bpy)(dafo\text{-}ketal)_2^{2+}$ (dotted line), $Ru(dafo\text{-}ketal)_3^{2+}$ (short dash line).

Results

UV−Visible Spectra of Complexes. The absorption spectra are illustrated in Figure 2, and energy maxima and absorption coefficients are summarized in Table 1. The absorption coefficients were obtained from Beer's law studies and determined from at least four dilution points. Two distinct sets of absorption bands were present for all of the ruthenium com-

(11) Demas, J. N.; Crosby, G. A. *J. Phys. Chem.* **1971**, *75*, 991.
(12) Cook, M. J.; Lewis, A. P.; McAuliffe, G. S. G.; Skarda, V.; Thomson, A. J.; Glasper, J. L.; Robbins, D. J. *J. Chem. Soc., Perkin Trans. 2* **1984**, 1293.
(13) *ORIGIN*, Version 3.78; MicroCal Software: Northampton, MA, 1991−3.

Table 1. Visible−UV Data for the Ruthenium Compounds[a]

complexes	λ_{max}, nm (ϵ, M^{-1} cm^{-1})			
$(bpy)_2Ru(dafo)^{2+}$	439 (1.5×10^4)	317 (1.8×10^4) (s)	285 (6.6×10^4)	240 (3.9×10^4)
$(bpy)Ru(dafo)_2^{2+}$	427 (1.4×10^4)	319 (2.5×10^4) (s)	288 (3.9×10^4)	236 (5.1×10^4)
$Ru(dafo)_3^{2+}$	419 (1.4×10^4)	317 (3.2×10^4) (s)	298 (4.0×10^4)	233 (6.0×10^4)
$(bpy)_2Ru(dafo\text{-}ketal)^{2+}$	445 (1.3×10^4)	317 (1.6×10^4) (s)	286 (7.5×10^4)	240 (2.5×10^4)
$(bpy)Ru(dafo\text{-}ketal)_2^{2+}$	444 (1.3×10^4)	312 (3.0×10^4) (s)	287 (4.5×10^4)	253 (1.3×10^4)
$Ru(dafo\text{-}ketal)_3^{2+}$	439 (1.3×10^4)	310 (4.5×10^4) (s)	297 (5.4×10^4)	
$Ru(bpy)_3^{2+}$	450 (1.4×10^4)		285 (8.7×10^4)	240 (3.0×10^4)

[a] In acetonitrile; $T = 23 \pm 1$ °C; $\lambda_{max} \pm 1$ nm; $\epsilon \pm 0.1$; s = shoulder.

Table 2. Redox Potentials for the Ruthenium Complexes[a]

compound	$E_{1/2}$, V (ΔE_p,[b] mV)						
	oxidations				reductions		
$(bpy)_2Ru(dafo)(PF_6)_2$	1.39 (78) [1.41][d]	−0.65 (61)			−1.34 (76) [−1.36]	−1.54 (96)	−1.78 (88)
$(bpy)Ru(dafo)_2(PF_6)_2$	1.52 (70) [1.53]	−0.62[c]	−0.68[c]		−1.34[c] [−1.40]	−1.52[c]	−1.78[c]
$Ru(dafo)_3(PF_6)_2$	1.64 (85)	−0.61[c]	−0.67[c]	−0.75[c]	−1.44[c]	−1.55[c]	−1.65[c]
$(bpy)_2Ru(dafo\text{-}ketal)(PF_6)_2$	1.29 (78) [1.36]				−1.33 (74) [−1.30]	−1.51 (78)	−1.76 (102)
$(bpy)Ru(dafo\text{-}ketal)_2(PF_6)_2$	1.41 (88) [1.43]				−1.27 (84) [−1.28]	−1.46 (124)	−1.66 (150)
$Ru(dafo\text{-}ketal)_3(PF_6)_2$	1.49 (76)				−1.26 (84)	−1.44 (98)	−1.62 (122)
$Ru(bpy)_3^{2+}$	1.28 (60)				−1.32 (60)	−1.52 (60)	−1.77 (60)

[a] All samples measured in 0.1 M TBAH/CH_3CN; error in potentials was ±0.02 V; $T = 23 \pm 1$ °C; scan rate = 100 mV/s; E_P in parentheses. [b] $\Delta E_p = E_{1/2(ox)} - E_{1/2(red)}$. [c] Waves overlap. [d] Calculated values in brackets—see text.

plexes. The probable assignments for the absorption bands were made on the basis of the well-documented optical transitions in $[Ru(bpy)_3]^{2+}$.[14] The set at higher energy can be attributed to intraligand $\pi \rightarrow \pi^*$ transitions; the set at lower energy can be assigned as metal-to-ligand charge transfer, $d\pi \rightarrow \pi^*$, transitions. The shapes of the $d\pi \rightarrow \pi^*$ transitions did not differ greatly among the complexes, but the positions of the $d\pi \rightarrow \pi^*$ transitions were blue-shifted compared to those of $[Ru(bpy)_3]^{2+}$. As the number of dafo ligands increased from 1 to 3 in the complexes, the MLCT bands shifted to higher energy in the sequence 439, 427, and 419 nm, respectively. As the number of dafo-ketal ligands increased from 1 to 3 in the complexes, the MLCT bands also shifted to higher energy in the sequence 445, 444, and 439 nm, respectively. In contrast to the MLCT bands, as the number of dafo ligands increased from 1 to 3 in the complexes, the $\pi \rightarrow \pi^*$ transitions shifted to lower energy in the sequence 285, 288, and 298 nm, respectively. A similar trend for the $\pi \rightarrow \pi^*$ transitions was also observed as the number of dafo-ketal ligands increased in the complexes. However, there was almost no difference in the $\pi \rightarrow \pi^*$ transition energies between the corresponding dafo and dafo-ketal complexes.

Electrochemistry. Reduction potentials for the complexes in CH_3CN were obtained by cyclic voltammetry and differential pulse polarography. Results are listed in Table 2. Reversibility was assessed on the basis of the oxidation/reduction peak spacings of 59/*n* mV, where *n* is the number of electrons transferred, and the ratios of i_{red}/i_{ox} which were near 1 for a reversible couple.[15] The number of electrons involved in a redox process was assessed by coulometry in selected cases and then by peak current comparisons. The assignments of ruthenium(III/II) couples and bipyridine ligand reductions were made on the basis of the well-established redox properties of ruthenium polypyridyl complexes.[2a,b]

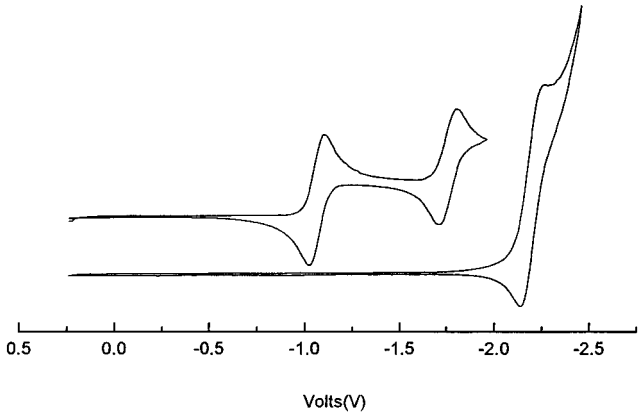

Figure 3. Cyclic voltammogram of the ligands dafo (up) and 2,2′-bipyridine (down) in acetonitrile at room temperature.

The cyclic voltammogram for the reduction of dafo is compared to the one for the reduction of bpy in Figure 3. Two reductions for dafo are located at −1.06 and −1.76 V compared to one for bpy located at −2.20 V.

The cyclic voltammogram of $[Ru(bpy)_2(dafo)]^{2+}$ and the differential pulse polarogram of $[Ru(dafo)_3]^{2+}$ in the negative region are shown in Figure 4 as examples. The oxidation corresponds to removal of an electron from the d orbital of Ru^{II} to give Ru^{III}. These fall in the 1.39−1.64 V range and shift to more positive potential as the number of dafo ligands increases. For the complex $[(bpy)_2Ru(dafo)]^{2+}$, the first two reductions at −0.65 ($n = 0.98$) and −1.34 V correspond to reduction of the dafo ligand and the third and fourth reductions for $[(bpy)_2Ru(dafo)]^{2+}$ correspond to subsequent reductions of the two bipyridine ligands. For $[(bpy)Ru(dafo)_2]^{2+}$, the peak positions at −0.62 and −0.68 V and at −1.38 and −1.52 V for the first and the second sequential reduction of each dafo ligand, respectively, were resolved by differential pulse measurements due to overlap within each set. The final reduction wave corresponds to reduction of the bipyridine ligand. For $[Ru(dafo)_3]^{2+}$, two sets of reductions were observed. The first set contained three reductions at −0.61, −0.67, and −0.75 V, and the second set contained three reductions located at −1.44, −1.55, and −1.65 V, which are all related to the reduction of

(14) (a) Rillema, D. P.; Taghdiri, D. G.; Jones, D. S.; Keller, C. D.; Worl, L. A.; Meyer, T. J.; Levy, H. A. *Inorg. Chem.* **1987**, *26*, 578. (b) Rillema, D. P.; Mack, K. B. *Inorg. Chem.* **1982**, *21*, 3849. (c) Rillema, D. P.; Callahan, R. W.; Mack, K. B. *Inorg. Chem.* **1982**, *21*, 2589.
(15) Christopher M. A. B.; Ana, M. O. B. *Electrochemistry: Principles, Methods, and Application*; Oxford University Press: New York, 1993.

Table 3. Emission Data for the Ruthenium Complexes[a,b]

	77 K		298 K			
complex	λ_{max}, nm	τ, ns[c]	λ_{max}, nm	τ, ns[c]	$10^4\Phi_{em}$[c]	λ_{max}(abs),nm
$(bpy)_2Ru(dafo)^{2+}$	568, 604	5280	638	312	12.8	447
$(bpy)Ru(dafo)_2^{2+}$	589, 606	4606	634	236	2.9	437
$Ru(dafo)_3^{2+}$	593, 637	3806	627	*d*	1.3	423
$(bpy)_2Ru(dafo\text{-}ketal)^{2+}$	567, 610	5102	600	586	130	447
$(bpy)Ru(dafo\text{-}ketal)_2^{2+}$	564, 611	3665	601	330	6.0	443
$Ru(dafo\text{-}ketal)_3^{2+}$	566, 607	1725	*d*	*d*	*d*	437
$Ru(bpy)_3^{2+}$	576, 622	5291	599	837	890	450

[a] $\lambda_{ex} = 436$ nm, ± 1 nm; λ_{max} ± 1 nm; freeze−pump−thaw degassed, unless otherwise noted. [b] Solvent: 4:1 EtOH−MeOH. [c] Values are $\pm 10\%$. [d] Too weak to measure.

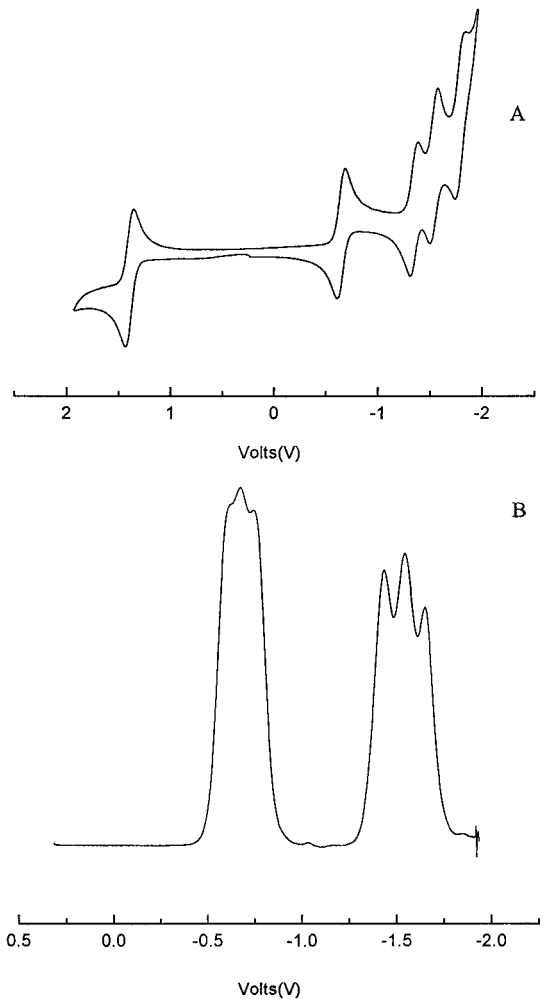

Figure 4. (A) Cyclic voltammogram of $[(bpy)_2Ru(dafo)]^{2+}$ in acetonitrile containing 0.1 M Bu_4NPF_6. (B) Differential pulse polarogram of $[Ru(dafo)_3]^{2+}$ in acetonitrile containing 0.1 M Bu_4NPF_6.

coordinated dafo ligands and resolved by differential pulse measurements due to overlap within each set.

The cyclic voltammograms and differential pulse polarograms of ruthenium ketal complexes were similar to those of $[Ru(bpy)_3]^{2+}$ with one oxidation and three reductions commencing near -1.23 V. Oxidations attributed to the $Ru^{III/II}$ potential ranged from 1.29 to 1.49 V as the number of ketal ligands increased. Compared to those of the dafo series, the oxidations were less positive. The intermediate reductions at > -1 V disappeared for the ketal derivatives, and the only reductions observed were a series of three corresponding to reduction of each bipyridine unit. These reductions occurred at more positive potentials than reduction of the bipyridine units in the dafo series. The energy associated with electrostatic interactions in the dafo series most likely shifted the second ligand reduction to more negative potential; hence, electrostatic repulsions can account for the observed differences in potentials between the dafo and dafo-ketal ligand reductions.

There is good agreement between the experimental $E_{1/2}$ values and those calculated using the methods proposed by Lever[16] in eqs 3 and 4, where n varies between 0 and 3. The parameter

$$E_{1/2}(\text{calc, dafo complexes}) = nE(\text{bpy}) + (3-n)E(\text{dafo}) \quad (3)$$

$$E_{1/2}(\text{calc, dafo-ketal complexes}) = nE(\text{bpy}) + (3-n)E(\text{dafo-ketal}) \quad (4)$$

E_L can be calculated as one-third the potential for the $[RuL_3]^{3+}/[RuL_3]^{2+}$ or $[RuL_3]^{2+}/[RuL_3]^{+}$ couples. Calculated $E_{1/2}$ values are then obtained by summing over all ligands. The calculated values are listed in Table 2 after the first oxidation and first "bipyridine" ligand reduction.

Emission Properties at 77 and 298 K. As shown in Figure 5, the emission spectra of the complexes at 77 K show vibrational components but are broad and less structured at 298 K, similar to those reported for $[Ru(bpy)_3]^{2+}$.[17] The positions of the first vibrational maxima obtained at 77 K and the emission maxima obtained in fluid solution at room temperature are listed in Table 3. For the $[(bpy)_nRu(dafo)_{3-n}]^{2+}$ complexes, the emission maxima at 77 K were 568, 589, and 593 nm as n decreased from 2 to 0. In contrast to the red shift at 77 K, the emission maxima at 298 K blue-shift from 638 to 634 and 627 nm, respectively. The red shift at 77 K is opposite the normal observation and may be related to increased delocalization of electron density as the number of dafo ligands increases, which becomes attenuated in fluid solution. In contrast to those of the dafo series, the positions of the emission energy maxima for $[(bpy)_nRu(dafo\text{-}ketal)_{3-n}]^{2+}$ ($n = 0-2$) are relatively constant at both 77 and 298 K but shifted about 33 nm from ~567 to ~600 nm upon changing from the glassy matrix at 77 K to fluid solution at room temperature.

Emission decays were monoexponential at both 77 and 298 K, and the results are given in Table 3. The emission lifetimes were approximately an order of magnitude larger in the glassy matrix at 77 K compared to fluid solution at room temperature. This variation is consistent with the metal-to-ligand charge-transfer nature of the process where solvent plays a critical role in responding to the photoinduced dipole change and thereby facilitates relaxation to the ground state.[18] At 77 K, the emission lifetimes fall in the following series: $[(bpy)_2Ru(dafo)]^{2+}$ (5280 ns) > $[(bpy)Ru(dafo)_2]^{2+}$ (4606 ns) > $[Ru(dafo)_3]^{2+}$ (3806 ns);

(16) Lever, A. B. P. *Inorg. Chem.* **1990**, *29*, 1271.
(17) (a) Hager, G. D.; Crosby, G. A. *J. Am. Chem. Soc.* **1975**, *97*, 7031. (b) Hager, G. D.; Watts, R. J.; Crosby, G. A. *J. Am. Chem. Soc.* **1975**, *97*, 7037.

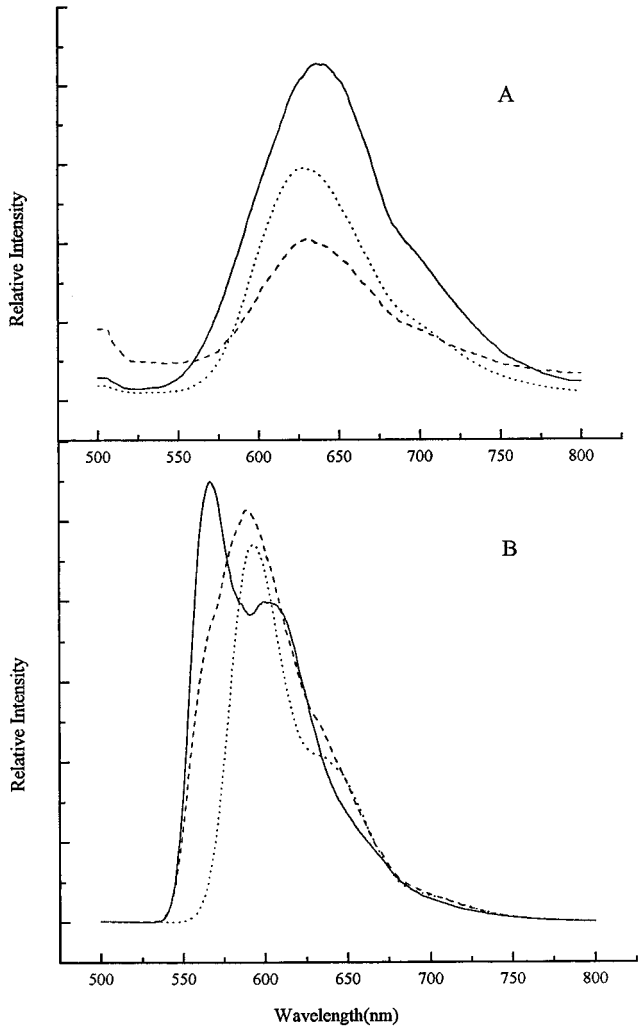

Figure 5. (A) Emission spectra of $Ru(bpy)_2(dafo)^{2+}$ (solid), $Ru(bpy)(dafo)_2^{2+}$ (dash), and $Ru(dafo)_3^{2+}$ (dot) at room temperature in 4:1 EtOH−MeOH. (B) Emission spectra of $Ru(bpy)_2(dafo)^{2+}$ (solid), $Ru(bpy)(dafo)_2^{2+}$ (dash), and $Ru(dafo)_3^{2+}$ (dot) at 77 K in 4:1 EtOH−MeOH.

$[(bpy)_2Ru(dafo\text{-}ketal)]^{2+}$ (5102 ns) > $[(bpy)Ru(dafo\text{-}ketal)_2]^{2+}$ (3665 ns) > $[Ru(dafo\text{-}ketal)_3]^{2+}$ (1725 ns). At 298 K, for $[(bpy)_nRu(dafo\text{-}ketal)_{3-n}]^{2+}$ complexes as n varies from 2 to 1, emission lifetimes are 586 and 330 ns, respectively. $[Ru(dafo\text{-}ketal)_3]^{2+}$ showed no detectable emission at room temperature. For the $[(bpy)_nRu(dafo)_{3-n}]^{2+}$ series, room-temperature emission lifetimes were in the order $[(bpy)_2Ru(dafo)]^{2+}$ (312 ns) > $[(bpy)Ru(dafo)_2]^{2+}$ (236 ns) > $[Ru(dafo)_3]^{2+}$ (none detectable).

The emission quantum yields for the complexes were determined relative to $[Ru(bpy)_3]^{2+}$ (0.089) at room temperature in a 4:1 ethanol−methanol mixture.[11] Emission quantum yields for the $[(bpy)_nRu(dafo)_{3-n}]^{2+}$ complexes decreased in the order $[(bpy)_2Ru(dafo)]^{2+}$ (12.8×10^{-4}) > $[(bpy)Ru(dafo)_2]^{2+}$ (2.9×10^{-4}) > $[Ru(dafo)_3]^{2+}$ (1.3×10^{-4}), while for the $[(bpy)_nRu(dafo\text{-}ketal)_{3-n}]^{2+}$ series the order was $[(bpy)_2Ru(dafo\text{-}ketal)]^{2+}$ (130×10^{-4}) > $[(bpy)Ru(dafo\text{-}ketal)_2]^{2+}$ (6.0×10^{-4}) > $[Ru(dafo\text{-}ketal)_3]^{2+}$ (none detectable).

Temperature-Dependent Emission Lifetimes. Emission lifetimes were measured at different temperatures in 4:1 ethanol−methanol over the 90−200 K range and are shown in Figure 6. Starting at 90 K, the emission lifetimes of a specific complex remained nearly the same in the glassy matrix but began to decrease through the glass-to-fluid region (~130 K). In the fluid region above 140 K, emission lifetimes decreased rapidly. The temperature-dependent lifetime behavior was fit to eq 2, and the results are given in Table 4. The barriers were much lower than those for $[Ru(bpy)_3]^{2+}$,[19] commencing at 1400 cm^{-1} for $[(bpy)_2Ru(dafo\text{-}ketal)]^{2+}$ and at 1150 cm^{-1} for $[(bpy)_2Ru(dafo)]^{2+}$ and decreasing by 60−70% within each series as the number of bipyridine ligands decreased.

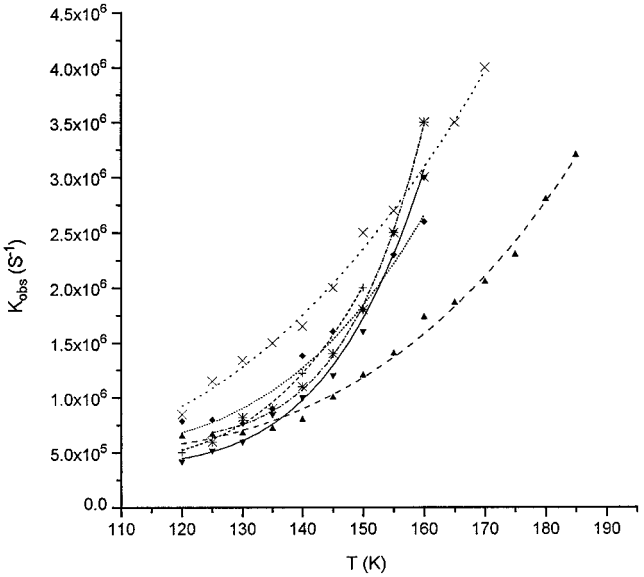

Figure 6. Emission lifetimes of $Ru(bpy)_2(dafo)^{2+}$ (▼), $Ru(bpy)(dafo)_2^{2+}$ (▲), $Ru(dafo)_3^{2+}$ (×), $Ru(bpy)_2(dafo\text{-}ketal)^{2+}$ (*), $Ru(bpy)(dafo\text{-}ketal)_2^{2+}$ (+), and $Ru(dafo\text{-}ketal)_3^{2+}$ (◆) as a function of temperature. The solvent is EtOH−MeOH (4:1).

Table 4. Data for Excited-State Decay Obtained by Temperature-Dependent Lifetime Measurements[a,b]

compound	k_o, s^{-1}	k_1, s^{-1}	ΔE, cm^{-1}
$(bpy)_2Ru(dafo)(PF_6)_2$	3.60×10^5	8.14×10^{10}	1147 ± 153
$(bpy)Ru(dafo)_2(PF_6)_2$	4.54×10^5	7.69×10^9	726 ± 58
$Ru(dafo)_3(PF_6)_2$	3.51×10^5	5.02×10^8	523 ± 61
$(bpy)_2Ru(dafo\text{-}ketal)(PF_6)_2$	6.02×10^5	8.93×10^{11}	1406 ± 89
$(bpy)Ru(dafo\text{-}ketal)_2(PF_6)_2$	3.51×10^5	1.42×10^{10}	944 ± 113
$Ru(dafo\text{-}ketal)_3(PF_6)_2$	4.77×10^5	2.63×10^9	789 ± 182

[a] λ_{ex} = 450 nm, ±1 nm; freeze−pump−thaw degassed, unless otherwise noted. [b] Solvent: 4:1 EtOH−MeOH.

Photosubstitution Processes. The complexes were examined for photosubstitution but appeared photochemically stable. Excitation under conditions known to lead to photosubstitution in ruthenium heterocyclic ligand complexes (λ_{ex} = 450 nm, 1 mM tetraethylammonium chloride, acetonitrile)[20] resulted in no changes in emission intensity, even over an extended irradiation period of several hours.

Discussion

Preparation of Compounds. Syntheses of ruthenium(II) heterocyclic ligand complexes starting with ruthenium(IV), ruthenium(III), and ruthenium(II) precursors have often been carried out in reducing solvents, such as ethanol. To provide enough thermal energy in the preparation and still maintain a

(18) (a) Kim, H.-B.; Kitamura, H.; Tazuke, S. *J. Phys. Chem.* **1990**, *94*, 1414. (b) Milder, S. J. *Inorg. Chem.* **1989**, *28*, 868. (c) Kitamura, N.; Sato, J.; Kim, H.-B.; Obota, R.; Tazuke, S. *Inorg. Chem.* **1988**, *27*, 651. (d) Kober, E. M.; Sullivan, B. P.; Meyer, T. J. *Inorg. Chem.* **1984**, *23*, 2098. (e) Caspar, J. V.; Meyer, T. J. *J. Am. Chem. Soc.* **1983**, *105*, 5583.

(19) Van Houten, J.; Watts, R. J. *J. Am. Chem. Soc.* **1976**, *98*, 4853.

(20) Durham, B.; Caspar, J. K.; Nagle, J. K.; Meyer, T. J. *J. Am. Chem. Soc.* **1982**, *104*, 4803.

Scheme 1. Ruthenium-Catalyzed Formation of dafo-ketal Complexes

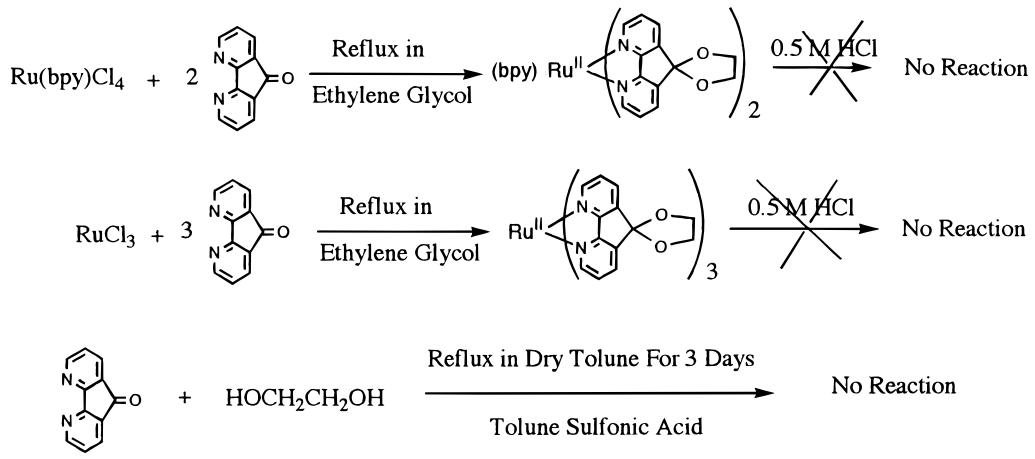

reducing environment, some of the syntheses have been carried out in ethylene glycol due to its high boiling point.[21] Reactions of $Ru(bpy)Cl_4$ (or $RuCl_3$) in ethylene glycol with a stoichiometric quantity of dafo resulted in the formation of $[Ru(bpy)(dafo\text{-}ketal)_2]^{2+}$ (or $[Ru(dafo\text{-}ketal)_3]^{2+}$). Formation of $[Ru(bpy)_2(dafo\text{-}ketal)]^{2+}$ required the presence of the catalyst *p*-toluenesulfonic acid, whereas the ketal derivatives of the other complexes formed without the catalyst. The free ligand dafo was unreactive in ethylene glycol. But $[Ru(bpy)(dafo)_2]^{2+}$ and $[Ru(dafo)_3]^{2+}$ reacted with ethylene glycol to generate the respective substituted ketal ligands, indicating ketal formation was related to the reaction of ethylene glycol with the coordinated dafo ligand. This type of reaction is often used to protect ketones in organic reactions; the ketals which form are then hydrolyzed to regenerate the ketone.[22] However these ruthenium dafo-ketal derivatives were stable to hydrolysis, even in refluxing 0.5 M HCl solutions. The above reactions are summarized in Scheme 1.

$[Ru(bpy)_2(dafo)]^{2+}$ was prepared in the traditional way by reaction of $Ru(bpy)_2Cl_2$ with dafo in ethanol. $[Ru(bpy)(dafo)_2]^{2+}$ was prepared by metathesis in ethanol as illustrated in eq 5. The procedure requires the prior preparation of the

$$Ru(bpy)Cl_4 + 4Ag(dafo)_2^{2+} \xrightarrow{\text{ethanol}} [Ru(bpy)(dafo)_2]^{2+} + 4AgCl + 6dafo \quad (5)$$

Ag^+ complex of the heterocyclic ligand and then its reaction with the appropriate ruthenium precursor.[23] The driving force in the reaction is precipitation of AgCl. The final compound in the series, $[Ru(dafo)_3]^{2+}$, was prepared by the reaction of $RuCl_3$ with dafo in nitrobenzene.

IR spectra showed carbonyl absorption bands located at about 1740 cm^{-1} for dafo complexes. For the ketal complexes, the carbonyl absorption band disappeared. New bands located at 1280 and 1213 cm^{-1} were observed and assigned to C−O stretching vibrations. The NMR spectra of bipyridine protons for both dafo and ketal complexes overlap with each other in the aromatic region. For dafo complexes, no aliphatic absorption band was found, while a single aliphatic absorption band located at about 4.5 ppm was observed for ketal complexes. There were no observable chemical shift changes for CH_2CH_2 protons among the ketal complexes.

At this point, one can only speculate about the reason for ketal formation and its stability to hydrolysis for the coordinated dafo ligand. One thing is clear: the electron density on the carbonyl group increases as noted by the increase in the C═O frequency from 1720 to 1740 cm^{-1} upon coordination of dafo to ruthenium(II). This change, however, would be expected to diminish nucleophilic addition of ethylene glycol to form the ketal. The stability may then be related to the rigidity of the ligand to torsional motion due to the attachment of the coordinating nitrogen atoms of the pyridine rings to the ruthenium center.

Electronic and Electrochemical Properties. The initial reduction in complexes containing the dafo ligand must be related to reduction of the coordinated dafo ligand. First, the free ligand undergoes two reductions, the first at −1.06 V and the second at −1.76 V. As found in other systems, these reductions shift positively by 0.4−0.5 V upon coordination to ruthenium(II).[24] Second, upon formation of the dafo-ketal ligand, the initial reduction at <-1.0 V disappears; the reductions for the dafo-ketal complexes follow the usual pattern for tris heterocyclic chelates of ruthenium(II).[25] Two possible assignments for the first reduction of dafo can be proposed. The first (**I**) assigns the added electron to the five-membered

I **II**

ring, generating a cyclopentadiene π system; the second (**II**) assigns the added electron density to the most electronegative atom, oxygen, and the unpaired electron to the carbonyl carbon atom. The former would delocalize electron density over the

(21) Blanton, C. B. M.S. Thesis, The University of North Carolina at Charlotte, 1990; see also references therein.
(22) (a) Alfred, H. *Organic Syntheses Based on Name Reactions and Unnamed Reactions*; Pergamon Press: New York, 1994. (b) March J. *Advanced Organic Chemistry: Reactions, Mechanisms, and Strucutre*, 4th ed.; John Wiley & Sons: New York, 1992.
(23) Kakoti, M.; Deb, A. K.; Goswami, S. *Inorg. Chem.* **1992**, *31*, 1302.
(24) Arana, C. A.; Abruna, H. D. *Inorg. Chem.* **1993**, *32*, 194.
(25) (a) Elliott, C. M.; Hershenhart, E. J. *J. Am. Chem. Soc.* **1982**, *104*, 7519. (b) Sahai, R.; Baucom, D. A.; Rillema, D. P. *Inorg. Chem.* **1986**, *25*, 3843. (c) Van Wallendael, S.; Shaver, R. J.; Rillema, D. P.; Yoblinski, B. J.; Stathis, M.; Guarr, T. *Inorg. Chem.* **1990**, *29*, 167. (d) Van Wallendael, S.; Perkovic, M. W.; Rillema, D. P. *Inorg. Chim. Acta* **1993**, *213*, 253.

Scheme 2. Reduction Sequences of the dafo Ligand

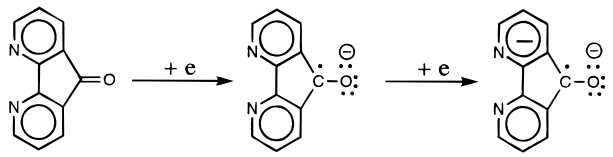

dafo ligand, resulting in one π system linking the carbonyl functionality, the five-membered ring, and the bipyridine π system into one unit; the latter would segregate the π system of the bipyridine ring from the carbonyl component; thus both would behave independently.

The first case can be supported by the increase in the C═O frequency shift from 1720 to 1740 cm^{-1} upon coordination. The shift is due to the positively charged metal center accepting electron density from the ligand, which strengthens the C═O bond slightly.

Several reasons can be cited to support the second case. First, the thermodynamic energy gap as judged by the difference in redox potential between electrochemical oxidation and electrochemical reduction of ruthenium complexes has been found to correlate with metal-to-ligand charge-transfer energy maxima.[26] This energy gap in the case of the dafo chelates is small, and one would expect to observe a low-energy absorption in the near-infrared spectrum associated with charge transfer from the ruthenium center to the carbonyl carbon atom. None is observed. Second, for the series of dafo and dafo-ketal complexes, a linear relationship is observed between the energy in cm^{-1} of the absorption assigned as the lowest energy MLCT transition and the thermodynamic energy gap in cm^{-1} as determined from the difference between the potential of the first oxidation and the potential of the first "bipyridine" ligand reduction. This correlation has a slope of 0.42 with an *R* value of 0.98. According to the data in Tables 1 and 2, the blue shift in the absorption spectra accompanying the decrease of *n* in the series $[Ru(bpy)_n(dafo)_{3-n}]^{2+}$ is related to stabilization of the Ru(II) dπ orbitals ($E_{1/2(ox)}$ becomes more positive; $E_{1/2(red)}$ remains nearly constant). The fact that $[Ru(dafo)_3]^{2+}$ and $[Ru(dafo\text{-}ketal)_3]^{2+}$ are included in this correlation would imply that the second reduction of the dafo ligand is related to reduction of the ligand's bipyridine π system, generating a biradical species as shown in Scheme 2. Third, emission properties are in accord with a triplet state associated with the "bipyridine" functionality in these complexes.

In summary, the evidence suggests the presence of resonance between strucures **I** and **II**. Structure **II**, however, seems to be the dominant one.

Excited-State Properties. The model for excited state deactivation is shown in Figure 7. Emission occurs from a triplet metal-to-ligand charge-transfer state populated by intersystem crossing from a singlet metal-to-ligand charge-transfer state. The temperature dependence of the emission lifetimes can be attributed to population of a triplet charge-transfer state due to the inertness of the complexes to photosubstitution, which suggests that the dd state does not play an important role in the deactivation process. This thermally accessible excited state most likely is the fourth metal-to-ligand charge transfer state (MLCT″) previously identified by Barbara[27] and Meyer and coworkers.[28]

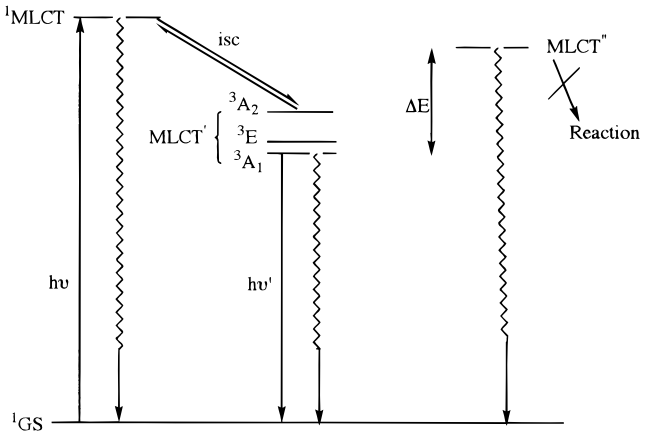

Figure 7. Energy state diagram based on a modified Crosby−Meyer model.

The presence of the carbonyl group does not appear to play a significant role in excited-state deactivation. It is clear from the absorption and emission data that there is little interaction between the metal dπ orbitals and the molecular orbitals of the carbonyl group. Filling the hole vacated by the promoted electron appears to be the preferential route for excited-state relaxation. Energetics favor this pathway by about 0.4 V.

An examination of the emission properties of the ruthenium complexes reveals some variations. For the ruthenium dafo-ketal series at 77 and 298 K, the emission lifetimes decrease as the bipyridine ligands are replaced with dafo-ketal ligands while the energy gap remains nearly constant. For the ruthenium dafo series, the behavior at 77 K differs from that at 298 K. At 77 K, the emission lifetimes decrease in concert with the energy gap as the bipyridine ligands are replaced with dafo ligands, but at 298 K, the opposite is true. In this case, the emission lifetimes decrease while the energy gap increases. In solution this effect can be attributed to the variation in the thermal energy gap as the number of dafo or dafo-ketal ligands increases, which causes an increase in the rate of decay to the ground state via the thermally accessible MLCT″ state. As pointed out by Meyer and co-workers, the energy gap law is correct only for nonradiative decay from the lowest MLCT state (or states).[29] In the ketal case at 77 K, thermal population of the MLCT″ state ($E_{thermal} \approx 50$ cm^{-1}) is unlikely. The increased number of ethylene glycol groups opens additional vibronic decay pathways and may account for the observations.

Calculations of k_r from emission lifetimes and emission quantum yields for $[Ru(bpy)_2(dafo)]^{2+}$, $[Ru(bpy)(dafo)_2]^{2+}$, $[Ru(dafo)_3]^{2+}$, and $[Ru(bpy)(dafo\text{-}ketal)_2]^{2+}$ yield values that are lower than expected for Ru(II) polypyridyl emitters ($\Phi_{em} = \tau k_r$, $k_r \approx 50\,000$ s^{-1}).[29] Although great efforts were made to avoid $[Ru(bpy)_3]^{2+}$ as an impurity by using $Ru(bpy)_2CO_3$ as the starting material with appropriate and repeated purification by ion exchange chromatography, the presence of $[Ru(bpy)_3]^{2+}$ impurities is still possible, especially since we have found that coordinated dafo ligands undergo nucleophilic ring opening to yield 3-substituted bipyridine ligands, resulting in complexes which emit strongly just like $[Ru(bpy)_3]^{2+}$.[3b]

Comparison to Ruthenium(II) Complexes with "Bipyridine" Ligands Derivatized in the 3,3′-Positions. Ruthenium-

(26) (a) Cloninger, K. K.; Callahan, R. W. *Inorg. Chem.* **1981**, *20*, 1611. (b) Lever, A. B. P.; Licoccia, S.; Magnell, K.; Minor, P. C.; Ramaswamy, B. S. *Adv. Chem. Ser.* **1982**, *No. 201*, 237. (c) Templeton, J. L. *J. Am. Chem. Soc.* **1979**, *101*, 4906. (d) Zwickel, A. M.; Creutz, C. *Inorg. Chem.* **1971**, *10*, 2395.

(27) Olson, E. J. C.; Hu, D.; Hormann, A.; Jonkman, A. M.; Arkin, M. R.; Stemp, E. D. A.; Barton, J. K.; Barbara, P. F. *J. Am. Chem. Soc.* **1997**, *119*, 11458.

(28) (a) Meyer, T. J. *Pure Appl. Chem.* **1990**, *62*, 1003. (b) Meyer, T. J. *Pure Appl. Chem.* **1986**, *58*, 1193.

(29) Treadway, J. A.; Loeb, B.; Lopez, R.; Anderson, P. A.; Keene, F. R.; Meyer, T. J. *Inorg. Chem.* **1996**, *35*, 2242.

(II) complexes containing bipyridine ligands derivitized in the 3,3′-positions behave much like their unsubstituted bipyridine ligand analogues, but with somewhat diminished emission.[2c,30] The closed six-membered-ring ligands fall in the 1,10-phenanthroline class, and the excited-state properties of their ruthenium(II) complexes are analogous to those containing the 2,2′-bipyridines.[2c,30] The complexes studied here contain closed five-membered rings attached in the 3,3′-positions and exhibit markedly diminished emission properties. The results can be compared directly to those for the ruthenium complex $[Ru(bpy)_2(diaz)]^{2+}$, where diaz is diazafluorene.[7,31] This complex displayed even weaker emission properties than the dafo or dafo-ketal complexes, and the weaker emission was attributed to populating a low-lying ligand field (LF) state, although photosubstitution was not examined to verify the postulate.

Acknowledgment. We thank the Office of Basic Energy Sciences of the Department of Energy for financial support, the National Science Foundation for the laser equipment, and Johnson Matthey for the loan of the source ruthenium compound.

IC970987E

(30) Kalyanasundaram, K. *Photochemistry of Polypyridine and Porphyrin Complexes*; Academic Press: New York, 1992.

(31) Wacholtz, W. M.; Auerbach, R. A.; Schmehl, R. H.; Ollino, M.; Cherry, W. R. *Inorg. Chem.* **1985**, *24*, 1758.